Acta Crystallographica Section D
Biological Crystallography
ISSN 0907-4449

Production and X-ray crystallographic analysis of fully deuterated cytochrome P450cam

Flora Meilleur,[a,b]* Marie-Thérèse Dauvergne,[a] Ilme Schlichting[c] and Dean A. A. Myles[a,d]*

[a]European Molecular Laboratory Grenoble Outstation, 6 Rue Jules Horowitz, 38042 Grenoble, France, [b]Institut Laue–Langevin, 6 Rue Jules Horowitz, BP156, 38042 Grenoble, France, [c]Abteilung Biomolekulare Mechanismen, Max-Planck-Institut für Medizinische Forschung, Jahnstrasse 29, 69120 Heidelberg, Germany, and [d]ORNL, PB 2008, Oak Ridge, TN 37831, USA

Correspondence e-mail: meilleur@ill.fr, mylesda@ornl.gov

Received 25 November 2004
Accepted 3 February 2005

PDB References:
hydrogenated cytochrome P450cam, 1yrc, r1yrcsf; deuterated cytochrome P450cam, 1yrd, r1yrdsf.

Neutron protein crystallography allows H-atom positions to be located in biological structures at the relatively modest resolution of 1.5–2.0 Å. A difficulty of this technique arises from the incoherent scattering from hydrogen, which considerably reduces the signal-to-noise ratio of the data. This can be overcome by preparing fully deuterated samples. Efficient protocols for routine and low-cost production of *in vivo* deuterium-enriched proteins have been developed. Here, the overexpression and crystallization of highly (>99%) deuterium-enriched cytochrome P450cam for neutron analysis is reported. Cytochrome P450cam from *Pseudomonas putida* catalyses the hydroxylation of camphor from haem-bound molecular O_2 *via* a mechanism that is thought to involve a proton-shuttle pathway to the active site. Since H atoms cannot be visualized in available X-ray structures, neutron diffraction is being used to determine the protonation states and water structure at the active site of the enzyme. Analysis of both hydrogenated and perdeuterated P450cam showed no significant changes between the X-ray structures determined at 1.4 and 1.7 Å, respectively. This work demonstrates that the fully deuterated protein is highly isomorphous with the native (hydrogenated) protein and is appropriate for neutron protein crystallographic analysis.

1. Introduction

Neutron protein crystallography can be used to directly visualize H-atom positions in biological structures at resolutions of 1.5–2.0 Å. This is because the neutron-scattering lengths of hydrogen and of its deuterium isotope are similar in magnitude to those of the 'heavy' atoms found in biological macromolecules (Table 1). The enhanced visibility of hydrogen and of its deuterium isotope in neutron protein structures allows the protonation state of key catalytic residues to be directly determined and allows detailed models of (heavy) water structure to be described (Bon *et al.*, 1999; Habash *et al.*, 2000; Coates *et al.*, 2001; Ostermann *et al.*, 2002; Kurihara *et al.*, 2004). A major hurdle in neutron diffraction is that unusually large crystals (>1 mm^3) are normally required to compensate for the weak flux of available neutron beams. Moreover, hydrogen has a large incoherent neutron-scattering cross-section that contributes to a large incoherent scattering background in neutron crystallography that often swamps the coherent (Bragg) diffraction from hydrogenous materials. In contrast, the incoherent scattering cross-section of deuterium is some 40 times lower (Table 1). The incoherent scattering background can therefore be largely overcome by deuterating the sample, either partially by soaking crystals in deuterated mother liquor or more fully by preparing completely

Table 1
Coherent scattering lengths and incoherent scattering cross-sections for atoms in biological macromolecules.

	H	D	C	N	O
B_{coh} (fm)	−3.74	+6.67	+6.65	+9.36	+5.81
σ_{coh} (barns)	1.76	5.59	5.56	11.03	4.23
σ_{inc} (barns)	80.27	2.05	0	0.49	0

(per)deuterated protein samples. In addition to the replacement of the bulk solvent and of hydration waters, exchange against deuterated solvent also enables H atoms that are bound to solvent-accessible N or O atoms to exchange with deuterium. This typically results in about 20% of the hydrogen content of the protein undergoing H/D exchange.

In order to replace H atoms that are covalently bound to carbon, it is necessary to express the protein under deuterated conditions. Protein expression in bacterial systems grown in media containing 100% D_2O gives maximal deuteration levels of ∼86% randomly distributed through the protein (Leiting *et al.*, 1998). Whilst such levels of deuterium labelling are now regularly used in NMR to reduce the spectral complexity for larger protein systems and in small-angle neutron scattering to label and highlight individual components in protein complexes, neutron protein crystallography is more demanding and requires levels of deuteration that ideally exceed 99%. This can be achieved by cell growth and expression using a deuterated carbon source in 100% D_2O, which provides deuterium-enrichment levels better than 99%. This high deuteration level offers critical benefits, principally in providing a tenfold improvement in signal-to-noise in neutron diffraction experiments (enabling smaller crystals and/or shorter time frames to be used), but also in enhancing the visibility of D atoms and water (D_2O) positions in the resulting maps (Shu *et al.*, 2000). Since the scattering length of deuterium is similar in sign and magnitude to those of C, N and O (Table 1), deuterium should be as visible as carbon at 2.0 Å resolution.

Previous reports of *in vivo* deuterium enrichment in *Escherichia coli* have relied upon commercially available (and expensive) rich media derived from bacterial hydrolysate that contain labelled amino acids and some low-molecular-weight oligopeptides (Tuominen *et al.*, 2004) or upon low-density cultivation in minimal medium (Shu *et al.*, 2000). We have established reliable protocols for high cell-density cultivation and expression of D-labelled protein using relatively low-cost perdeuterated minimal media (Meilleur *et al.*, 2004). Such minimal media are easily prepared from heavy water, perdeuterated glycerol and essential mineral salts and can give higher biomass yield than rich media when coupled with high cell-density cultivation techniques.

We are using a combined high-resolution X-ray and neutron crystallographic approach to determine the specific hydration states and hydrogen-bonding networks at the active site of P450cam. Cytochromes P450 (P450s) are haem-containing monooxygenases found throughout the biosphere (for a comprehensive review of all aspects of P450, see Ortiz de Montellano, 1995). P450s play diverse functional roles in a broad range of biological systems. In mammals, they are involved in a wide variety of biochemical processes including carcinogenesis, drug metabolism, biosynthesis of lipids and steroids or degradation of xenobiotics. They catalyse a two-electron activation of O_2, resulting in the formation of a water molecule and the insertion of a single O atom into the substrate. Addition of the first electron reduces the haem iron to the ferrous state to which molecular oxygen can bind. Addition of the second electron that reduces the P450–O_2 complex is combined with a critical proton transfer at the active site that leads to cleavage of the O—O bond.

Cytochrome P450cam (CYP101) from the soil bacteria *Pseudomonas putida* is the monooxygenase responsible for the stereospecific and regiospecific hydroxylation of camphor when used as sole carbon source. Numerous studies aiming to elucidate the critical details of the proton-delivery pathway involved in the O_2 activation have been performed over the last decades. The X-ray crystallographic structures of individual intermediates of the reaction pathway have now been determined at high resolution (Poulos *et al.*, 1986, 1987; Li *et al.*, 1995; Schlichting *et al.*, 2000). This structural information combined with complementary biophysical studies and site-directed mutagenesis experiments (Vidakovic *et al.*, 1998; Westlake *et al.*, 1999; Hishiki *et al.*, 2000; Deng *et al.*, 2001) has allowed the determination of some essential structural properties of the P450cam active site and provided critical insights into understanding important steps in the enzymatic mechanism. Mutagenesis studies have demonstrated that the highly conserved residues Asp251 and Thr252 play a key role and it was postulated that their side chains could be involved in the proton delivery required for catalytic activity. However, the P450cam–O_2 X-ray structure determined by Schlichting *et al.* (2000) suggests that Asp251 and Thr252 are indirectly involved in the proton-delivery pathway, stabilizing two catalytic waters (W901 and W902) that are only observed at the active site upon O_2 binding (Fig. 1). Water molecules W901 and W902 may then actually shuttle protons to O_2 through an internal water channel composed of three additional water molecules W523, W566 and W687 (Schlichting *et al.*, 2000). In this mechanism, W901 is the final O_2 proton donor. The resolution of the currently available X-ray structures does not allow direct visualization of the H-atom positions in the protein and the organization of the hydrogen-bonding network at the active site remains ambiguous. Therefore, the hydrogen-shuttle pathway is still a matter of debate.

The enhanced visibility of hydrogen and of its deuterium isotope in neutron protein structures suggests that neutron protein crystallography could provide critical information on W901 and W902 orientations, on their hydrogen-bonding interactions with Asp251 and Thr252, and on the protonation state of Asp251 that could help further characterize the proton-shuttle pathway in the P450cam enzymatic mechanism. However, at 47 kDa P450cam is a relatively large system for neutron analysis, containing some 3282 heavy atoms and 3232 H atoms. Since only ∼22% of the protein H atoms could be H/D-exchanged *via* crystal soaking in deuterated mother liquor and since even a 5% H contamination significantly

Table 2
Minimal medium composition.

Component	Initial concentration
KH_2PO_4	13.3 g l^{-1}
$(NH_4)_2HPO_4$	4.0 g l^{-1}
Citric acid	1.7 g l^{-1}
$MgSO_4{\cdot}7H_2O$	1.2 g l^{-1}
Trace-metal solution†	1 ml l^{-1}
Thiamine.HCl	4.5 mg l^{-1}
Glycerol	5 g l^{-1}

† 6 g l^{-1} Fe^{III} citrate, 1.5 g l^{-1} $MnCl_2{\cdot}4H_2O$, 0.8 g l^{-1} $Zn(CH_3COO)_2{\cdot}2H_2O$, 0.3 g l^{-1} H_3BO_3, 0.2 g l^{-1} $Na_2MoO_4.2H_2O$, 0.25 g l^{-1} $CoCl_2{\cdot}6H_2O$, 0.15 g l^{-1} $CuCl_2{\cdot}2H_2O$, 0.84 g l^{-1} EDTA.

reduces the gain offered by deuteration (Gamble *et al.*, 1994), we have overexpressed fully deuterated P450cam using high cell-density cultivation techniques. Both hydrogenated and deuterated P450cam have been expressed, purified and crystallized in several different crystal forms. We report here the preliminary X-ray analysis of hydrogenated and (per)deuterated P450cam crystals in the tetragonal $P4_32_12$ space group, including comparison of overall structure and, critically, report that the protein conformation and the water structure near the active site are isomorphous in the hydrogenated and deuterated forms.

2. Experimental procedures

2.1. P450cam expression in high cell-density cultures

P450cam was overexpressed in *Escherichia coli* BL21 (DE3) cells using high cell-density cultivation (HCDC) techniques (Lee, 1996; Riesenberg & Guthke, 1999) following protocols closely similar to those previously described (Meilleur *et al.*, 2004). We note the following differences. Optimal expression was obtained using the medium described by Riesenberg *et al.* (1991) (Table 2). Cultures were performed in 2 l fermenters (Infors) and after a batch phase at close to maximum growth rate, glycerol was added to maintain a constant but limited growth rate ($\mu < \mu_{max}$) controlled by monitoring the increase of dissolved oxygen and pH variations (Riesenberg & Guthke, 1999). In hydrogenated media, cells were harvested 24 h after induction at a final OD_{600} of 25, yielding ∼70 g of wet cell paste per ∼50 g of hydrogenated glycerol provided and approximately 1 g of hydrogenated P450cam in the apoprotein form.

For expression of (per)deuterated protein, *E. coli* cells were adapted to growth in fully deuterated medium in a three-step procedure on plated media at 310 K (Meilleur, 2004; Meilleur *et al.*, 2004). Adapted cells were transferred to fully deuterated liquid media and grown for 2 d. We note that cycling this step by inoculating fresh media in a 1:20 ratio increases the initial growth rate. D-adapted cells were either used directly to inoculate large-scale fermenter solutions or flash-frozen in 10 ml aliquots and stored at 193 K for future use. In deuterated media, cells were harvested 40 h after induction at a final OD_{600} of 7.0, yielding ∼15 g of wet cell paste per 13.2 ml of perdeuterated glycerol provided and ∼90 mg of deuterated P450cam in the apoprotein form.

Table 3
Data-collection, processing and refinement statistics for hydrogenated and perdeuterated $P4_32_12$ crystals.

Values in parentheses are for the last shell.

	Hydrogenated P450cam	Perdeuterated P450cam
Molecular weight (Da)	46797	50053
Temperature (K)	100	100
X-ray source	ID14 (EH4)	BM14
Wavelength	0.939	0.992
Detector	ADSC Q4 CCD	MAR CCD
Space group	$P4_32_12$	$P4_32_12$
Unit-cell parameters (Å)		
$a = b$	63.7	63.4
c	246.5	248.6
Resolution (Å)	20–1.4	20–1.7
Completeness (%)	99.8 (99.1)	98.7 (84.6)
Multiplicity	6.5 (3.3)	7.5 (3.50
$I/\sigma(I)$	7.8 (2.7)	4.8 (2.3)
R_{sym}† (%)	4.9 (31.6)	7.7 (27.9)
Non-H atoms		
Protein	3208	3208
Haem	43	43
Camphor	11	11
Solvent	489	357
R_{free}/R_{work}† (%)	21.9/20.2	21.3/19.8
R.m.s. deviations from ideal value		
Bond lengths (Å)	0.005	0.005
Bond angles (°)	1.34	1.33
Mean B factors (Å^2)		
Main-chain atoms	16.4	19.1
Side-chain atoms	18.6	20.8
Haem	11.3	14.8
Camphor	12.6	19.9
Potassium ion	13.0	17.0
Solvent atoms	27.9	30.2

† $R_{sym} = \sum |I - \langle I \rangle|/I$. † $R_{work} = \sum |F_{obs}| - k|F_{calc}|/\sum |F_{obs}|$.

2.2. Purification of hydrogenated and perdeuterated P450cam

The hydrogenated and the deuterated apoprotein were purified as described previously (Meilleur *et al.*, 2004). The haem-reconstruction procedure was adapted from previously described protocols (Auclair *et al.*, 2001). The protein integrity was confirmed by an absorbance ratio (392/280 nm) of 1.4. All purification steps were performed in H_2O buffers. For the deuterated P450cam, exchangeable H atoms were back-exchanged to deuteriums against deuterated crystallization buffer (50 m*M* Tris–DCl pH_{meas} 7.4, 250 m*M* KCl, 1 m*M* camphor, 100 m*M* DTE).

2.3. Crystallization and X-ray data collection

Tetragonal and orthorhombic hydrogenated crystals were grown by microdialysis following the procedure described by Schlichting *et al.* (1997). Deuterated crystals were grown under closely similar conditions. 25 µl deuterated protein solution (7.5–30 mg ml^{-1}) was dialysed against 2 ml 50 m*M* Tris–HCl pH_{meas} 7.4, 250 m*M* KCl, 1 m*M* camphor, 100 m*M* DTE and 14–18% polyethylene glycol (PEG) 8000 at 277 K. Crystals grew within 5 d from various crystallization solutions. Tetragonal bipyramids of up to 1 mm in size were grown from a 7.5 mg ml^{-1} protein solution dialysed against 18% PEG 8000.

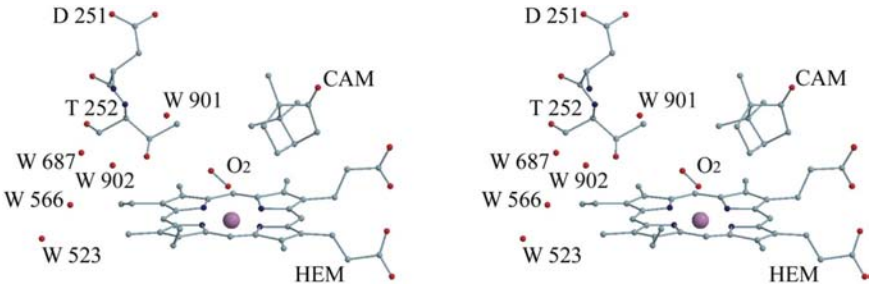

Figure 1
Positions of the catalytically important residues Asp251 and Thr252 and the critical water positions W901 and W902 in the P450cam–O_2 crystal structure (PDB code 1dz8; Schlichting *et al.*, 2000).

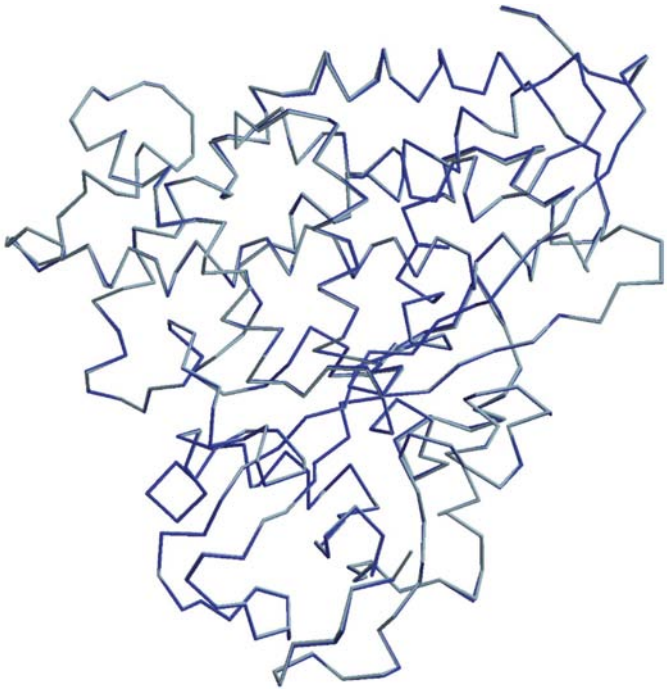

Figure 2
Superposition of $P4_32_12$ hydrogenated and perdeuterated P450cam backbone structures. Light blue, hydrogenated P450cam; blue, perdeuterated P450cam.

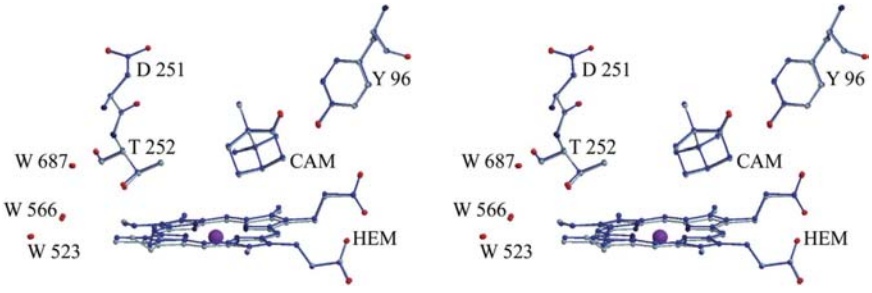

Figure 3
Superposition of the active site showing the hydrogen bound between Tyr96 and the camphor carbonyl O atom, the Asp251 and Thr252 key residues and the internal water channel (W523, W566 and W687). Light blue, hydrogenated P450cam; blue, perdeuterated P450cam.

Orthorhombic needles were grown from a 22.5 mg ml^{-1} protein solution dialysed against 16% PEG 8000. The crystals were cryoprotected by passing them through mother liquor supplemented with 20% glycerol (d_8-glycerol for the deuterated crystal) immediately before cooling to 100 K in an N_2-gas stream on the beamline.

3. Results

3.1. Deuteration level

The deuteration level of the sample was determined by mass spectrometry. A tryptic digest of deuterated P450cam was analysed by TOF MS ES+. The software *Isotopic Pattern Calulator* v.1.6.5 for Macintosh (http://www.shef.ac.uk/chemistry/chemputer/isotopes.html) was used to calculate the theoretical isotopic pattern matching the experimental spectrum. This analysis corresponds to a deuteration level of 99.5%.

3.2. X-ray analysis

Synchrotron data were recorded at the ESRF beamlines ID14 and BM14. Data were processed and scaled using *MOSFLM* and *SCALA* (Collaborative Computational Project, Number 4, 1994). The tetragonal crystal form belongs to space group $P4_32_12$. The needles belong to the orthorhombic space group $P2_12_12_1$ (Schlichting *et al.*, 1997). We have collected and analysed complete X-ray data sets for both forms. We report here an analysis of the hydrogenated and deuterated crystals of the tetragonal form. Data-collection and analysis statistics for the hydrogenated and perdeuterated crystals are summarized in Table 3.

3.3. Structure determination and refinement

We have determined the 1.4 Å hydrogenated and 1.7 Å perdeuterated P450cam X-ray structures by molecular replacement using *MOLREP* (Vagin & Teplyakov, 1997). The structure of Poulos *et al.* (1987) (PDB code 2cpp) was used as a search model. Both structures were refined with *CNS* (Brünger *et al.*, 1998) (Table 3). The overall structure of the oxidized P450cam complex in the tetragonal form closely resembles the search model, with only minor conformational changes of surface side-chain residues. The overall (main chain and side chains) r.m.s. deviation between the hydrogenated and perdeuterated structures

is 0.6 Å, falling to 0.2 Å for the backbone atoms alone (Fig. 2). Critically, the detailed side chain and water structures at the active site are highly isomorphous between the hydrogenated and perdeuterated proteins. For the haem and the camphor the r.m.s. differences are 0.2 and 0.1 Å, respectively. The single hydrogen bond that holds the camphor in place between its carbonyl O atom and the side chain of Tyr96 is conserved in the hydrogenated and perdeuterated structures (2.7 Å compared with 2.9 Å in 2cpp and 2.5 Å in 1dz4) (Fig. 3). The conformations of the key residues Asp251 and Thr252 are maintained (overall r.m.s. 0.1 Å). The conserved light (H_2O) and heavy (D_2O) water positions are closely similar in the hydrogenated and perdeuterated crystal forms. In particular, the heavy waters 523, 566 and 687 (Poulos *et al.*, 1987) are located within 0.1 Å of the light water positions (Fig. 3).

4. Discussion and concluding remarks

Fully perdeuterated P450cam from *P. putida* has been expressed, purified and crystallized. Mass-spectrometry analysis has shown that our deuteration protocol leads to a high level of deuteration (>99%). This confirms that perdeuterated protein can be readily overexpressed using *E. coli* once optimal conditions have been well defined under hydrogenated conditions (Gamble *et al.*, 1994; Cooper *et al.*, 1998; Shu *et al.*, 2000). Moreover, we note that the final cell density is dependent primarily upon the total amount of d-glycerol provided. In our study, the expression level in perdeuterated media is decreased by a factor of 2–3 compared with the level of expression in hydrogenated media.

We note that whilst perdeuteration has subtle effects upon the physicochemical properties of proteins (Yokogaki *et al.*, 1995; Brockwell *et al.*, 2001; Meilleur *et al.*, 2004), the crystallization conditions for perdeuterated P450cam were readily re-optimized from the hydrogenated conditions using minimal amounts of perdeuterated material. Although there are few examples in the literature, we anticipate this to be a general feature of perdeuterated proteins (Gamble *et al.*, 1994; Cooper *et al.*, 1998; Shu *et al.*, 2000). In addition, and most critically for this and future neutron diffraction studies, any differences between the physicochemical properties of the hydrogenated and deuterated P450cam are not reflected in their structures, which are highly isomorphous at the resolution (1.7 Å) of this analysis. The ability to produce deuterium-labelled proteins routinely and in high yield is likely to underpin the future use and application of neutron crystallography to the determination of critical H-atom positions in biological macromolecules.

The recent surge in atomic resolution X-ray protein structure determinations (<1.2 Å) has helped emphasize and highlight the additional information and insight provided when H-atom positions can be determined experimentally. In cases where atomic resolution cannot be obtained, or where mobility renders H atoms still difficult to discern, neutron diffraction can offer a complementary approach to the determination of critical H-atom positions in protein structures. We have reported here a comparison of hydrogenated and perdeuterated P450cam structures in the $P4_32_12$ form as a preliminary to detailed neutron analysis. In addition, large perdeuterated crystals of the orthorhombic form ($P2_12_12_1$, $a = 63.21$, $b = 63.93$, $c = 105.64$ Å) have also been grown ($2.5 \times 0.2 \times 0.2$ mm after one month). This crystal form diffracted X-rays to 1.7 Å. The smaller unit-cell parameters are more favourable for neutron diffraction analysis. Therefore, we are optimizing the crystallization conditions of this form in order to improve the crystal habit and volume. The solution of the neutron P450cam and P450cam–O_2 structures should provide the most detailed models yet available for the hydration state and hydrogen-bonding interactions at the active site in P450 enzymes.

We are grateful to Stephen G. Sligar for providing the initial P450cam clone, and Michael Haertlein and Christiane Jung for helpful discussion concerning cloning and expression and purification of the protein. We thank the ILL/EMBL staff of the Deuteration Laboratory, Grenoble, France for assistance, Thomas Franz and Xinping Li (EMBL, Germany) for the mass-spectrometry analysis, and Sean McSweeney and Hassan Belrhali at ESRF (Grenoble, France) for help in data collection.

References

Auclair, K., Moënne-Loccoz, P. & Ortiz de Montellano, P. R. (2001). *J. Am. Chem. Soc.* **123**, 4877–4885.
Bon, C., Lehmann, M. S. & Wilkinson, C. (1999). *Acta Cryst.* D**55**, 978–987.
Brockwell, D., Yu, L., Cooper, S., McCleland, S., Cooper, A., Attwood, D., Gaskell, S. J. & Barber, J. (2001). *Protein Sci.* **10**, 572–580.
Brünger, A. T., Adams, P. D., Clore, G. M., DeLano, W. L., Gros, P., Grosse-Kunstleve, R. W., Jiang, J.-S., Kuszewski, J., Nilges, M., Pannu, N. S., Read, R. J., Rice, L. M., Simonson, T. & Warren, G. L. (1998). *Acta Cryst.* D**54**, 905–921.
Coates, L., Erskine, P. T., Wood, S. P., Myles, D. A. A & Cooper, J. B. (2001). *Biochemistry*, **40**, 13149–13157.
Collaborative Computational Project, Number 4 (1994). *Acta Cryst.* D**50**, 760–763.
Cooper, S. J., Brockwell, D., Raftery, J., Attwood, D., Barber, J. & Helliwell, J. R. (1998). *Chem. Commun.*, pp. 1063–1064.
Deng, T.-J., Macdonald, I. D. G., Simianu, M. C., Sykora, M., Kincaid, J. R. & Sligar, S. G. (2001). *J. Am. Chem. Soc.* **123**, 269–278.
Gamble, T. R., Clauser, K. R. & Kossiakoff, A. A. (1994). *Biophys. Chem.* **54**, 15–26.
Habash, J., Raftery, J., Nuttall, R., Price, H. J., Wilkinson, C., Kalb (Gilboa), A. J. & Helliwell, J. R. (2000). *Acta Cryst.* D**56**, 541–550.
Hishiki, T., Shimada, H., Nagano, S., Egawa, T., Kanamori, Y., Makino, R., Park, S.-Y., Adachi, S.-I., Shiro, Y. & Ishimura, Y. (2000). *J. Biochem.* **128**, 965–974.
Kurihara, K., Tanaka, I., Chatake, T., Adams, M. W., Jenney, F. E. Jr, Moiseeva, N., Bau, R. & Niimura, N. (2004). *Proc. Natl Acad. Sci. USA*, **101**, 11215–11220.
Lee, S. Y. (1996). *Trends Biotechnol.* **14**, 98–105.
Leiting, B., Marsilio, F. & O'Connell, J. F. (1998). *Anal. Biochem.* **265**, 351–355.
Li, H., Narasimhulu, S., Havran, L. M., Winkler, J. D. & Poulos, T. L. (1995). *J. Am. Chem. Soc.* **117**, 6297–6299.
Meilleur, F. (2004). Thesis. University J. Fourier, Grenoble, France.
Meilleur, F., Contzen, J., Myles, D. A. A. & Jung, C. (2004). *Biochemistry*, **43**, 8744–8753.

Ortiz de Montellano, P. R. (1995). Editor. *Cytochrome P450: Structure, Mechanism and Biochemistry*, 2nd ed. New York: Plenum.
Ostermann, A., Tanaka, I., Engler, N., Niimura, N. & Parak, F. G. (2002). *Biophys. Chem.* **95**, 183–193.
Poulos, T. L., Finzel, B. C. & Howard, A. J. (1986). *Biochemistry*, **25**, 5314–5322.
Poulos, T. L., Finzel, B. C. & Howard, A. J. (1987). *J. Biol. Chem.* **195**, 687–700.
Riesenberg, D. & Guthke, R. (1999). *Appl. Microbiol. Biotechnol.* **51**, 422–430.
Riesenberg, D., Schulz, V., Knorre, W. A., Pohl, H.-D., Korz, D., Sanders, E. A., Ross, A. & Decker, W.-D. (1991). *J. Biotechnol.* **20**, 17–28.
Schlichting, I., Berendzen, J., Chu, K., Stock, A. M., Maves, S. A., Benson, D. E., Sweet, R. M., Ringe, D., Petsko, G. A. & Sligar, S. G. (2000). *Science*, **286**, 1615–1622.
Schlichting, I., Jung, C. & Schulze, H. (1997). *FEBS Lett.* **415**, 253–257.
Shu, F., Ramakrishnan, V. & Schoenborn, B. P. (2000). *Proc. Natl Acad. Sci. USA*, **97**, 3872–3877.
Tuominen, V. U., Myles, D. A. A., Dauvergne, M.-T., Lahti, R., Heikinheimo, P. & Goldman, A. (2004). *Acta Cryst.* D**60**, 606–609.
Vagin, A. & Teplyakov, A. (1997). *J. Appl. Cryst.* **30**, 1022–1025.
Vidakovic, M., Sligar, S. G., Li, H. & Poulos, T. L. (1998). *Biochemistry*, **7**, 9211–9219.
Westlake, A. C. G., Harford-Cross, C. F., Donovan, J. & Wong, L.-L. (1999). *Eur. J. Biochem.* **265**, 929–935.
Yokogaki, S., Unno, K., Oku, N. & Okada, S. (1995). *Plant Cell Physiol.* **36**, 419–423.